Acta Crystallographica Section B
Structural Science
ISSN 0108-7681

X-ray crystal structures of diacetates of 6-s-*cis* and 6-s-*trans* astaxanthin and of 7,8-didehydroastaxanthin and 7,8,7′,8′-tetradehydroastaxanthin: comparison with free and protein-bound astaxanthins

Giuditta Bartalucci,[a] Stuart Fisher,[a] John R. Helliwell,[a] Madeleine Helliwell,[a]* Synnøve Liaaen-Jensen,[b] John E. Warren[c] and James Wilkinson[a]

[a]School of Chemistry, University of Manchester, Manchester M13 9PL, England, [b]Department of Chemistry, Norwegian University of Science and Technology, Trondheim, Norway, and [c]Daresbury Laboratory, Warrington, Cheshire WA4 4AD, England

Correspondence e-mail: madeleine.helliwell@manchester.ac.uk

Received 15 December 2008
Accepted 9 February 2009

The crystal structures of the 6-s-*cis* [s-*cis*-(1)] and 6-s-*trans* [s-*trans*-(1)] conformers of the diacetates of astaxanthin (AXT) and those of (3*S*,3′*S*)-7,8-didehydroastaxanthin [(3*S*,3′*S*)-3,3′-dihydroxy-7,8-didehydro-β,β-carotene-4,4′-dione (2)] and (3*S*,3′*S*)-7,8,7′,8′-tetradehydroastaxanthin [(3*S*,3′*S*)-3,3′-dihydroxy-7,8,7′,8′-tetradehydro-β,β-carotene-4, 4′-dione (3)] are reported. The conformations of these four molecules vary in particular with the angle of twist of the end rings out of the plane of the polyene chain; for s-*cis*-(1), the end rings are twisted out of the plane of the polyene chain by an angle of −49.0 (5)°, and the conformation is therefore similar to that found for unesterified AXT as well as for the carotenoids, canthaxanthin and β,β-carotene. For s-*trans*-(1), the end rings are coplanar with the polyene chain and its conformation is much more similar to that of the protein-bound AXT in the blue protein, crustacyanin, which is found in the shell of lobsters, although s-*trans*-(1) shows much less bowing of the polyene chain. In (2) and (3) the end rings are also almost coplanar with the polyene chain with the end rings in (2) in the s-*cis* conformation, and in (3) in the s-*trans* conformation. Thus, an extensive ensemble of the possible β end-ring conformations has been determined. These structures are compared with one another as well as unbound, unesterified AXT and protein-bound AXT. Also, the effect of the end-ring conformations on the colour and UV–vis spectra of the crystals was established.

1. Introduction

There has been considerable interest and speculation as to why, when a lobster is cooked, it changes from a dark slate blue colour, to bright red. It is now known that the chromophore responsible for the colour of the lobster is the carotenoid astaxanthin, AXT (3,3′-dihydroxy-β,β-carotene-4,4′-dione), which is found in the protein α-crustacyanin (α-CR; Cianci *et al.*, 2002; Chayen *et al.*, 2003; Zagalsky, 2003; Nneji & Chayen, 2004). The crystal structure of β-CR, which is a dissociation product of α-CR, consisting of two apo-protein sub-units and two AXT molecules, was determined in 2002 (Cianci *et al.*, 2002). This showed that the two AXT molecules are in close proximity, approaching to within 7 Å, adopt the 6-s-*trans* conformation, with the end rings approximately coplanar with the polyene chains, and are each hydrogen bonded to the protein *via* the keto O atoms to a bound water molecule at one end, and a histidine N atom at the other end (Cianci *et al.*, 2002).

The UV–vis spectrum of AXT in hexane shows a maximum absorption at 470 nm, whereas β-CR and α-CR in aqueous

buffer solution absorb at 585 and 630 nm, respectively. A number of different theories have been put forward as to how this very large bathochromic shift occurs (Weesie *et al.*, 1997; Durbeej & Eriksson, 2003, 2004; van Wijk *et al.*, 2005; Ilagen *et al.*, 2005). These include:

(i) the increased conjugation arising from coplanarization of the β-end rings with the polyene chain,

(ii) an electronic polarization effect stemming from hydrogen bonding to the keto O atoms (Weesie *et al.*, 1997; Durbeej & Eriksson, 2003, 2004), and

(iii) exciton coupling arising from the close proximity of the two bound astaxanthins (van Wijk *et al.*, 2005; Ilagan *et al.*, 2005).

Recently, we have begun complementary investigations to the protein-structure studies, whereby these different candidate tuning parameters are explored by obtaining more precise crystal structures of free carotenoids, including AXT, and the closely related molecules, canthaxanthin (β,β-carotene-4,4′-dione) and (3*R*,3′*S*, *meso*)-zeaxanthin [(3*R*,3′*S*)-β,β-carotene-3,3′-diol; Bartalucci *et al.*, 2007). In all these cases, the molecules were found to adopt the 6-s-*cis* conformation. The main difference between the conformations arose from the torsion angle between the polyene chain and the end rings which varied by a small amount (from −43 to −53°) for all the structures except (3*R*,3′*S*, *meso*)-zeaxanthin, where this angle was quite different at −74.9 (3)°. Although the crystals were all distinctly red in colour (and clearly not blue as for α- or β-CR; Zagalsky, 2003; Nneji & Chayen, 2004), the solid-state UV–vis spectrum of zeaxanthin was shifted slightly to a shorter wavelength compared with the other carotenoid crystals (Bartalucci *et al.*, 2007), owing to the reduced conjugation of the polyene chain into the end rings.

Here we report the crystal structures of the 6-s-*cis* [s-*cis*-(1)] and 6-s-*trans* [s-*trans*-(1)] conformers of the diacetates of AXT and those of (3*S*,3′*S*)-7,8-didehydroastaxanthin [(3*S*,3′*S*)-3,3′-dihydroxy-7,8-didehydro-β,β-carotene-4,4′-dione (2)] and (3*S*,3′*S*)-7,8,7′,8′-tetradehydroastaxanthin [(3*S*,3′*S*)-3,3′-dihydroxy-7,8,7′,8′-tetradehydro-β,β-carotene-4, 4′-dione (3); Fig. 1]. The acetylenic analogues, (2) and (3), are red/orange pigments found as the major carotenoids in starfish, such as *Asterias rubens*, and are also encountered in other marine animals; they are similar to AXT except for the presence of triple bonds between the C7 and C8 positions in the carbon backbone for (2) and the C7 and C8, and C7′ and C8′ positions for (3). The crystal structures of s-*trans*-(1), (2) and (3) were found to be quite different to those of s-*cis*-(1) and the other free carotenoids, AXT, canthaxanthin, zeaxanthin and β-carotene, with the end rings almost coplanar with the polyene chains, and with s-*trans*-(1) and (3) in the s-*trans* conformation, and (2) in the s-*cis* conformation. These new crystal structures are compared with the previously determined crystal structures of AXT and related carotenoids, as well as the structure of AXT found in the protein β-CR.

2. Experimental

2.1. Preparation of 6-s-*cis* and 6-s-*trans* astaxanthin diesters, s-*cis*-(1) and s-*trans*-(1)

The preparation was adapted from the method described by Karrer & Jucker (1950). To a solution of synthetic, optically inactive astaxanthin, containing a 1:2:1 mixture of the 3*R*,3′*R*:3*R*,3′*S*, *meso*:3*S*,3′*S* isomers, obtained from Sigma Chemicals (0.030 g, 0.05 mmol) in pyridine, was added acetic anhydride (0.04 ml, 0.5 mMol) with stirring in darkness for 4 h at room temperature. Then the solvent was removed by vacuum distillation. Flash chromatography (EtOAc:petroleum 1:4) gave astaxanthin monoester (0.016 g, 48.8%) and astaxanthin diester (0.015 g, 42.3%) as red powders. Plate crystals of both the *cis* and *trans* conformers of the astaxanthin diesters s-*cis*-(1) and s-*trans*-(1) were obtained in the same vial, by vapour diffusion from pyridine/H_2O and were separated by hand; the crystals of the *cis* conformer from pyridine/water were solvated with water. Later, improved crystals of s-*cis*-(1), solvated with ethyl acetate, were obtained from ethyl acetate/hexane, by vapour diffusion techniques, and the ethyl acetate

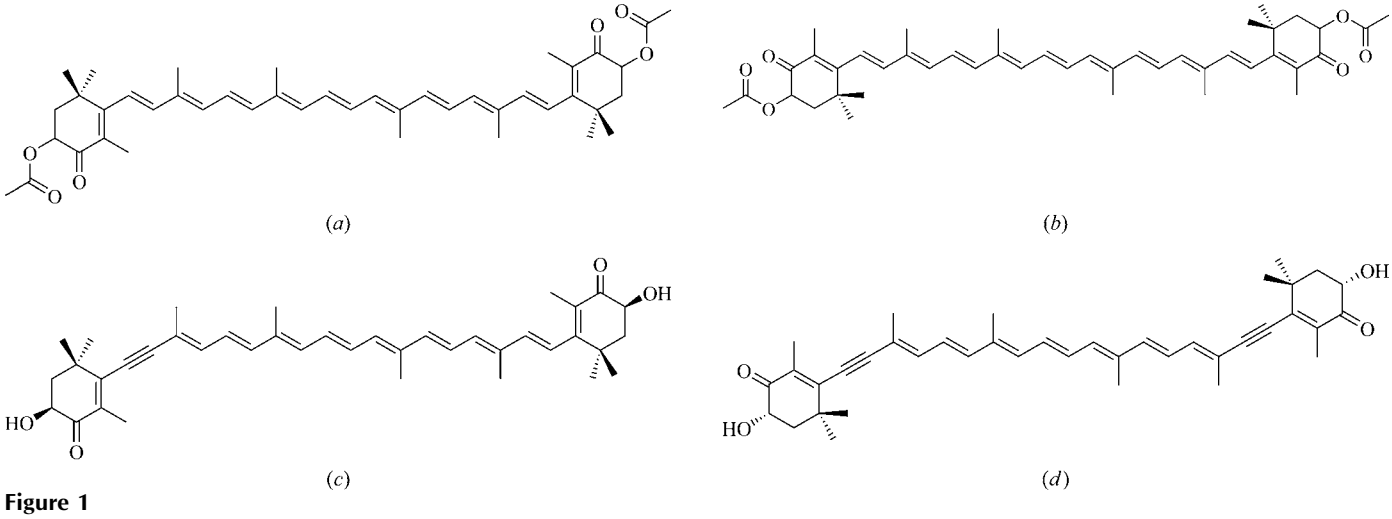

Figure 1
Chemical diagrams of (*a*) the s-*cis* conformer of astaxanthin diacetate, s-*cis*-(1); (*b*) the s-*trans* conformer of astaxanthin diacetate, s-*trans*-(1); (*c*) (3*S*,3′*S*)-7,8-didehydroastaxanthin (2); (*d*) (3*S*,3′*S*)-7,8,7′,8′-tetradehydroastaxanthin (3).

Table 1
Experimental details.

	s-*cis*-(1)	s-*trans*-(1)	(2)	(3)
Crystal data				
Chemical formula	$C_{44}H_{56}O_6 \cdot 0.44C_4H_8O_2$	$C_{44}H_{56}O_6$	$C_{40}H_{50}O_4$	$C_{40}H_{48}O_4$
M_r	719.59	680.89	594.80	592.78
Cell setting, space group	Monoclinic, $C2/c$	Monoclinic, $P2_1/c$	Triclinic, $P\overline{1}$	Triclinic, $P\overline{1}$
Temperature (K)	100	100	100	100
a, b, c (Å)	12.967 (2), 10.788 (1), 30.264 (4)	10.660 (1), 10.168 (1), 18.294 (2)	7.7821 (4), 9.9578 (5), 11.4162 (5)	7.477 (1), 10.473 (2), 11.633 (2)
α, β, γ (°)	90, 101.796 (1), 90	90, 100.700 (2), 90	88.126 (1), 78.329 (1), 84.340 (1)	75.606 (2), 85.901 (2), 76.389 (2)
V (Å^3)	4144.3 (8)	1948.4 (3)	862.08 (7)	857.5 (3)
Z	4	2	1	1
D_x (Mg m^{-3})	1.153	1.161	1.146	1.148
Radiation type	Mo $K\alpha$	Mo $K\alpha$	Synchrotron, λ = 0.6709 Å	Synchrotron, λ = 0.6710 Å
μ (mm^{-1})	0.08	0.08	0.07	0.07
Crystal form, colour	Plate, orange	Plate, red	Plate, red	Plate, red
Crystal size (mm)	0.60 × 0.60 × 0.05	0.60 × 0.60 × 0.10	0.2 × 0.2 × 0.02	0.04 × 0.03 × 0.01
Data collection				
Diffractometer	Bruker APEX CCD area detector	Bruker APEX CCD area detector	Bruker APEXII CCD area detector	Bruker APEXII CCD area detector
Data collection method	φ and ω scans	φ and ω scans	φ and ω scans	φ and ω scans
Absorption correction	None	None	Multi-scan†	Multi-scan†
T_{min}	–	–	0.736	0.749
T_{max}	–	–	1.000	1.000
No. of measured, independent and observed reflections	13 064, 3632, 2913	9816, 3425, 2506	6688, 3029, 2910	14 633, 4002, 2799
Criterion for observed reflections	$I > 2\sigma(I)$	$I > 2\sigma(I)$	$I > 2\sigma(I)$	$I > 2\sigma(I)$
R_{int}	0.076	0.072	0.016	0.062
θ_{max} (°)	25.0	25.0	23.8	26.1
Refinement				
Refinement on	F^2	F^2	F^2	F^2
$R[F^2 > 2\sigma(F^2)]$, $wR(F^2)$, S	0.085, 0.218, 1.11	0.065, 0.175, 1.08	0.046, 0.126, 1.08	0.042, 0.105, 1.01
No. of reflections	3632	3425	3029	4002
No. of parameters	304	305	428	409
H-atom treatment	Constrained‡	Constrained‡	Constrained‡	Constrained‡
Weighting scheme	$w = 1/[\sigma^2(F_o^2) + (0.0625P)^2 + 15.0678P]$, where $P = (F_o^2 + 2F_c^2)/3$	$w = 1/[\sigma^2(F_o^2) + (0.0489P)^2 + 1.5414P]$, where $P = (F_o^2 + 2F_c^2)/3$	$w = 1/[\sigma^2(F_o^2) + (0.0747P)^2 + 0.1591P]$, where $P = (F_o^2 + 2F_c^2)/3$	$w = 1/[\sigma^2(F_o^2) + (0.0581P)^2]$, where $P = (F_o^2 + 2F_c^2)/3$
$(\Delta/\sigma)_{max}$	< 0.0001	0.001	< 0.0001	0.003
$\Delta\rho_{max}$, $\Delta\rho_{min}$ (e Å^{-3})	0.54, −0.28	0.39, −0.21	0.17, −0.16	0.19, −0.17

Computer programs used: *SMART* (Bruker, 2001*a*), *SAINT* (Bruker, 2002), *SHELXS*97, *SHELXL*97 (Sheldrick, 2008), *SHELXTL* (Bruker, 2001*c*), *PLATON* (Spek, 2003). † Based on symmetry-related measurements. ‡ Constrained to parent site.

solvate is the crystal structure of s-*cis*-(1) reported here. The water and the ethyl acetate solvates of s-*cis*-(1) are isomorphous, but differ with respect to the incorporation of the disordered solvent molecules.

Samples of synthetic, optically pure (3*S*,3′*S*)-(2) and (3*S*,3′*S*)-(3) (Bernhard *et al.*, 1980) were obtained from Hoffmann–La Roche, Basle, and recrystallized from acetone/water and dichloromethane/hexane, respectively, by vapour-diffusion techniques, the latter at 278 K.

2.2. UV–vis spectra measurements

UV–vis spectra were measured on a Varian Cary 5000 UV–vis–NIR spectrometer. The solution-state spectra were recorded with the carotenoids dissolved in chloroform. The solid-state spectra were obtained from crystals pressed between two glass coverslips.

2.3. Determination of the X-ray crystal structures

Data collection for s-*cis*-(1) and s-*trans*-(1) was carried out using a Bruker APEX CCD diffractometer, using Mo $K\alpha$ radiation. For (2) and (3), the crystals were so small and weakly diffracting that synchrotron radiation from Station 9.8 at the SRS Daresbury Laboratory was necessary for the data collection. The crystal structures were solved by direct methods. The crystal data for all four crystal structures are summarized in Table 1.[1]

[1] Supplementary data for this paper are available from the IUCr electronic archives (Reference: RY5026). Services for accessing these data are described at the back of the journal.

For s-*cis*-(1) there was found to be disorder of the atoms O3, O4, O21, C1, C2, C3, C4, C16, C17, C21 and C22, where the larger fraction refined to an occupancy of 0.745 (4). Restraints were applied to the geometry of the lower-fraction component. There is a partially occupied ethyl acetate molecule, whose occupancy refined to a value of 0.22, and which was fixed at this value for the final rounds of refinement; some restraints were applied to its geometry.

For s-*trans*-(1), there is static disorder of the atoms O1, O3, O21, C1, C2, C3, C16, C17, C21 and C22, where the larger fraction refined to an occupancy of 0.788 (4). Restraints were applied to the geometry of the lower-fraction component.

In the case of (2), disorder was seen of the C7, C8, C7*B* and C8*B* atoms arising from an averaging of the acetylenic and olefenic positions at either end of the polyene chain; the occupancy of the higher component refined to a value of 0.64 (2). The H atoms bonded to C17 were modelled as two disordered components rotated by 60° from one another [occupancy of the higher component = 0.64 (2)]. Restraints were applied to the atomic displacement parameters of the disordered atoms.

For (2) and (3), although *ADDSYM* (*PLATON*; Spek, 2003) suggested additional symmetry up to the space group $P\bar{1}$, since the molecules are chiral, the refinement of the structures in the centrosymmetric space group was found to be unsatisfactory, with *R* values well above 0.2, thus confirming that the samples were indeed pure enantiomers. Since the hand could not be determined by anomalous dispersion techniques for these light atom structures using synchrotron radiation of wavelength of ~ 0.67 Å, the correct absolute configuration was assigned to be (3*S*,3′*S*) for each structure as they were known to be from enantioselective total synthesis.

Generally the non-H atoms were refined anisotropically, except some of those of the lower-occupancy components of the disordered atoms. H atoms were included in calculated positions and allowed to ride on their parent atoms. Hydroxyl H atoms were idealized and a rotating group refinement was employed so as to maximize the electron density, using the AFIX 147 command (Sheldrick, 2008). Methyl group H atoms were idealized using the AFIX 137 command (Sheldrick, 2008), which varies the torsion angle to maximize the electron density at the three H-atom positions.

3. Description of the structures

3.1. s-*cis*-(1) and s-*trans*-(1)

Chemical diagrams of both the astaxanthin diacetate conformers, s-*cis*-(1) and s-*trans*-(1), are shown in Figs. 1(*a*) and (*b*), and plots of the crystal structures are displayed in Figs. 2(*a*) and (*b*). In the crystal structures of each, the asymmetric unit consists of half the molecule, with the whole molecule being generated by an inversion symmetry operation. There is static disorder of the end rings of each conformer, arising from the presence of a 1:2:1 mixture of the three optical isomers of astaxanthin (3*S*,3′*S*; 3*R*,3′*S*, *meso*; 3*R*,3′*R*) in the synthetic material used in the preparation of s-*cis*-(1) and s-*trans*-(1); the extent of the disorder in each case is similar with the major components refining to occupancy values of 0.743 (4) and 0.788 (4), respectively, rather than to the statistically expected value of 0.5, presumably due to a preferential selection of isomers in the crystallization. Indeed this is in contrast to the crystal structures of the three crystal forms of AXT, where the ratio of the different conformations

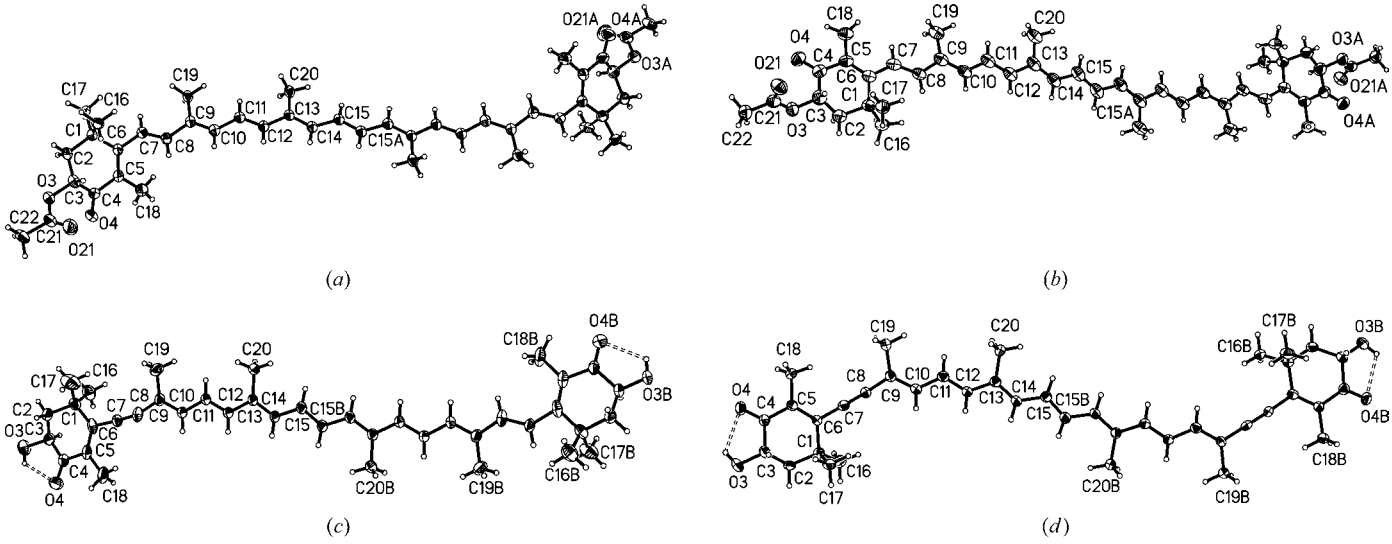

Figure 2
(*a*) Plot of the s-*cis* conformer of astaxanthin diacetate [s-*cis*-(1)] using 50% probability ellipsoids; only the higher-occupancy disordered component is shown and solvent molecules are omitted for clarity. (*b*) Plot of the s-*trans* conformer of astaxanthin diacetate [s-*trans*-(1)] using 50% probability ellipsoids; only the higher-occupancy disordered component is shown. (*c*) Plot of (3*S*,3′*S*)-7,8-didehydroastaxanthin (2) using 50% probability ellipsoids; only the higher-occupancy disordered component is shown. Hydrogen bonds are shown with dashed lines. (*d*) Plot of (3*S*,3′*S*)-7,8,7′,8′-tetradehydroastaxanthin (3) using 50% probability ellipsoids. Hydrogen bonds are shown with dashed lines.

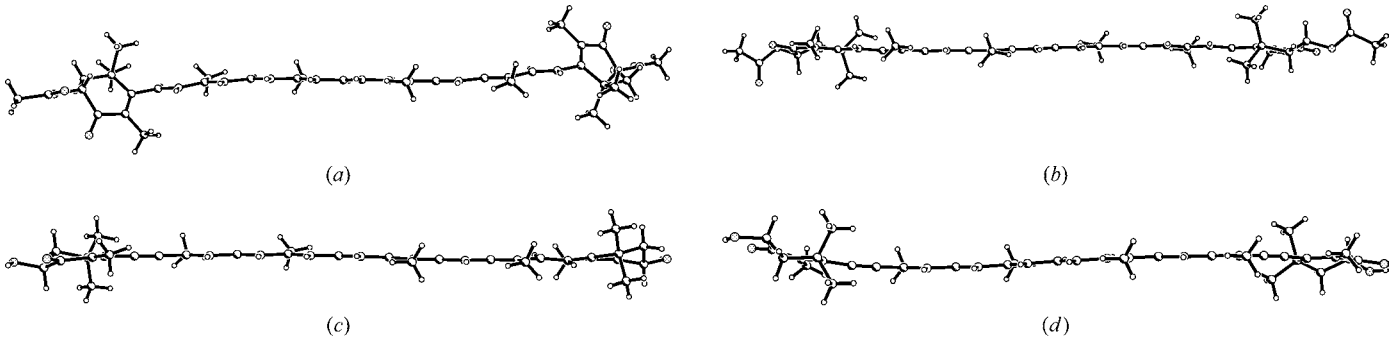

Figure 3
Plots of the molecules viewed down the planes of the polyene chains (*a*) of the s-*cis* conformer of astaxanthin diacetate, s-*cis*-(1); only the higher-occupancy disordered component is shown and solvent molecules are omitted for clarity; (*b*) of the s-*trans* conformer of astaxanthin diacetate, s-*trans*-(1); only the higher-occupancy disordered component is shown; (*c*) of (3*S*,3′*S*)-7,8-didehydroastaxanthin (2); only the higher-occupancy disordered component is shown; (*d*) of (3*S*,3′*S*)-7,8,7′,8′-tetradehydroastaxanthin, (3).

of the end rings was found to be approximately 1:1 (Bartalucci *et al.*, 2007).

In general, the geometric parameters of s-*cis*-(1) and s-*trans*-(1) agree closely with each other and with those of non-esterified AXT. In the case of s-*cis*-(1), the C5—C6—C7—C8 torsion angle, which gives a measure of the twisting of the end rings out of the plane of the polyene chain, was found to be −49.0 (5)°, similar to those found for AXT as well as the carotenoids canthaxanthin and *β*,*β*-carotene, where this angle ranges from about −43 to −53° (Bartalucci *et al.*, 2007). This is illustrated in Fig. 3(*a*), which is viewed down the plane of the polyene chain, clearly showing the twist of the end rings of s-*cis*-(1) out of the plane of the polyene chain. Moreover, calculations for the carotenoids AXT, canthaxanthin, zeaxanthin and *β*,*β*-carotene (Hashimoto *et al.*, 2002) predicted that the most favourable conformation of the end rings for these related carotenoids would be between −45 and −50°. For s-*trans*-(1), this angle is completely different at 178.3 (3)°, indicating that the end rings are basically coplanar with the polyene chain (Fig. 3*b*), a conformation predicted to be the least favourable of the possible conformations (Hashimoto *et al.*, 2002). The results presented here indicate that packing forces in the crystals of s-*trans*-(1) are presumably 'trapping' (*i.e.* stabilizing) this conformation in the crystal. An overlay of the polyene chains of the s-*cis*-(1) and s-*trans*-(1) crystal structures using the program *OFIT* is shown in Fig. 4 (Bruker, 2001*a*,*b*,*c*); the r.m.s. deviation is only 0.089 Å, indicating that the polyene chains are very similar to one another, but Fig. 4 clearly illustrates the differently oriented end rings.

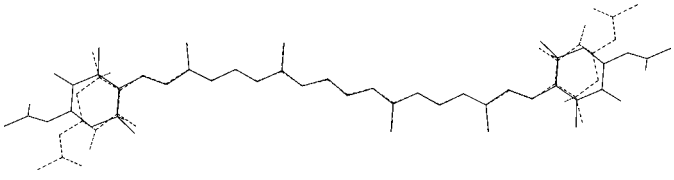

Figure 4
Overlay of the s-*cis* (dashed) and s-*trans* conformers of astaxanthin diacetate showing the similarity of their polyene chains, but difference of their end rings.

3.1.1. Packing. For s-*cis*-(1) there are no intermolecular hydrogen-bonding interactions, but there is possible weak *π*-stacking of the polyene chains one above the other, with a minimum distance of adjacent chains of C13–C13 (symmetry equivalent $-x, -y+1, -z+1$) of 3.942 (4) Å (Fig. 5). For s-*trans*-(1), there are two weak intermolecular C—H···O hydrogen-bonding interactions (Table 2, Fig. 6). The C22···O4 contact is a pair-wise interaction linking the molecules into chains, which are further linked into sheets *via* the C17···O4 linkage. The molecules do not show *π*-stacking, since the shortest contact between the polyene chains is 4.181 (4) Å (symmetry equivalent $-x+1, -y, -z$).

3.2. 7,8-Didehydroastaxanthin (2) and 7,8,7′,8′-tetradehydroastaxanthin (3)

Chemical diagrams of (2) and (3) are shown in in Figs. 1(*c*) and (*d*), and the crystal structures of (2) and (3) are illustrated in Figs. 2(*c*) and (*d*). Both crystallize in the space group *P*1 with one molecule in the unit cell and both show intramolecular hydrogen bonding of the hydroxyl groups with the adjacent keto O atoms. In (2) there is static disorder of the C7/C8 and C7*B*/C8*B* sites arising from the possibility of the acetylenic linkage being at one or other end of the polyene chain. Although (2) is in the s-*cis* conformation, the end rings are close to being coplanar with the polyene chains; since the torsion angle normally used to give the angle between the end ring and the polyene chain involves a linear acetylenic linkage, the value of the angle of twist of the end rings was instead estimated by calculating the dihedral angles between the least-squares planes through the C1, C4–C6 atoms and the C6, C9–C13 polyene chain atoms, and the C1*B*, C4*B*–C6*B* atoms and the C6*B*, C9*B*–C13*B* polyene chain atoms, for each end ring, giving values of 5.6 (1) and 10.3 (2)°, respectively. That the end rings are so close to being coplanar with the polyene chain is in contrast with the other s-*cis* carotenoids, AXT, canthaxanthin and zeaxanthin (Bartalucci *et al.*, 2007) as well as s-*cis*-(1), where this torsion angle is generally −43 to −53°, and −75.9 (4)° for zeaxanthin. For (3), the angles between the C1, C4–C6 (C1*B*, C4*B*–C6*B*) atoms and the C6, C9–C13 (C6*B*, C9*B*–C13*B*) polyene chain atoms are 13.3 (1) and 3.0 (1)°,

Table 2
Hydrogen bonds for s-*trans*-(1) (Å, °).

D—H···A	$d(D$—H)	d(H···A)	$d(D\cdots A)$	$\angle(DHA)$
C17—H17B···O4^{i}	0.98	2.58	3.510 (8)	158
C22—H22B···O4^{ii}	0.98	2.52	3.310 (6)	137

Symmetry codes: (i) $2-x, -y, 1-z$; (ii) $2-x, 1/2+y, 1/2-z$.

Table 3
Hydrogen bonds for (2) (Å, °).

D—H···A	$d(D$—H)	d(H···A)	$d(D\cdots A)$	$\angle(DHA)$
O3—H3···O4	0.82	2.27	2.671 (3)	111
O3B—H3B···O4B	0.82	2.19	2.651 (3)	116
C2—H2B···O3B^{i}	0.97	2.54	3.440 (4)	154
C15—H15···O4^{ii}	0.93	2.54	3.446 (3)	164
C17B—H17D···O4^{iii}	0.96	2.54	3.446 (4)	157

Symmetry codes: (i) $x+3, y+2, z-1$; (ii) $x-1, y-1, z+1$; (iii) $x-2, y-2, z+1$.

Table 4
Hydrogen bonds for (3) (Å, °).

D—H···A	$d(D$—H)	d(H···A)	$d(D\cdots A)$	$\angle(DHA)$
O3—H3···O4	0.82	2.17	2.649 (3)	118
O3B—H3B···O4B	0.82	2.19	2.629 (3)	114
C3B—H3B1···O4^{i}	0.98	2.36	3.141 (4)	136

Symmetry codes: (i) $x-1, y-1, z-2$.

respectively, again showing that the end rings are close to being coplanar with the polyene chains.

Overlay of the central portions of the polyene chains of (2) and (3) (r.m.s. deviation 0.11 Å; Fig. 7) shows that the positions of the end rings are quite different, and that they are s-*cis* for (2), and s-*trans* for (3).

3.2.1. Packing. In both (2) and (3), O3 and O3B form intramolecular hydrogen bonds with the adjacent keto O atoms, O4 and O4B (Figs. 2*c* and *d*), and there are no classical intermolecular hydrogen-bonding interactions. For (2), there are three weak intermolecular C—H···O hydrogen-bonding interactions linking the molecules into chains in three different directions leading to a three-dimensional network (Table 3, Fig. 8). There are no short contacts suggestive of π-stacking interactions. For (3), there is a weak intermolecular C—H···O hydrogen-bonding interaction between C3B and O4 (symmetry equivalent $x-1, y-1, z-2$), linking the molecules into chains (Table 4) as well as π-stacking between the adjacent polyene chains with shortest contact of 3.439 (4) Å between C11 and C9B (symmetry equivalent $x+1, y, z+1$), see Fig. 9.

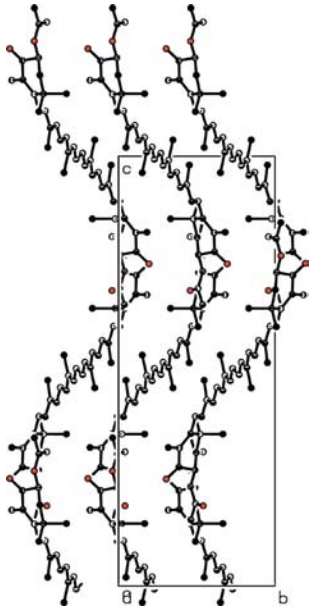

Figure 5
Packing of the s-*cis* conformer of astaxanthin diacetate, s-*cis*-(1), viewed approximately down **a**, showing the π-stacking interactions of the polyene chains; only the higher-occupancy disordered component is shown and solvent molecules and H atoms are omitted for clarity.

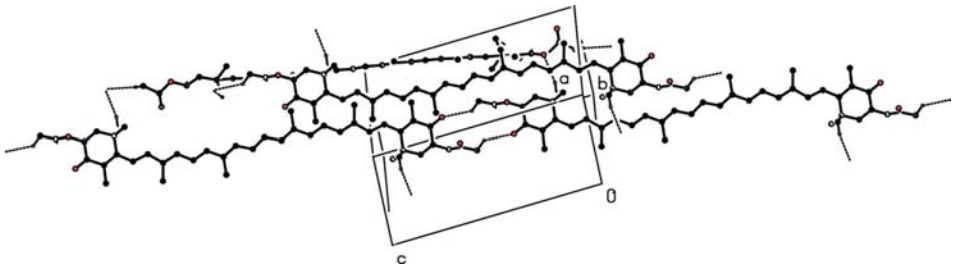

Figure 6
Packing of the s-*trans* conformer of astaxanthin diacetate s-*trans*-(1), showing the C—H···O hydrogen-bonding interactions; only the higher-occupancy disordered component and H atoms that are involved in the hydrogen bonding are shown.

4. Discussion

In our previous paper (Bartalucci *et al.*, 2007) we obtained much more precise structural parameters of AXT and related carotenoids than the protein crystal structure of β-CR at 3.2 Å (Cianci *et al.*, 2002) could provide. In addition we investigated how the conformation of the carotenoid, and particularly the angle of twist of the end rings to the plane of the polyene chain, as well as the crystal-packing arrangements, affected the colours of the crystals. We found that all the carotenoids crystallized in the s-*cis* conformation, with an angle of twist, given by the C5—C6—C7—C8 torsion angle, of −43 to −53° for AXT, canthaxanthin and β-carotene, but −74.9 (3)° for zeaxanthin, which led to a slight shift of the UV–vis absorption spectrum to shorter wavelength for

the latter crystals arising from the reduced conjugation into the end rings. Also, although a variety of packing modes was seen, the intermolecular interactions in the crystals did not affect the colours of the crystals significantly. However, in none of these crystal structures were the end rings in the s-*trans* conformation nor were they coplanar with the polyene chains, as they are in the protein-bound AXT in β-CR.

We decided to investigate the effect of the end-ring conformation on the colour of the crystals further, by preparing diesters of AXT by reaction of AXT with acetic anhydride, since their crystals were described as being blue in colour (Karrer & Jucker, 1950). Recrystallization yielded red crystals (although the crystals do appear dark blue in the bulk) of both the 6-s-*cis* [s-*cis*-(1)] and 6-s-*trans* [s-*trans*-(1)] conformers of the acetate diesters, allowing us to directly compare s-*cis* and s-*trans* conformers of the same molecule, both in terms of structure and the colour of the crystals. In addition, we determined the crystal structures of 7,8-didehydroastaxanthin (2) and 7,8,7′,8′-tetradehydroastaxanthin (3), which are found to be in the s-*cis* and s-*trans* conformations, respectively, with the end rings approximately coplanar with the polyene chains. Thus, these four crystal structures, together with the previously determined carotenoid crystal structures (Bartalucci *et al.*, 2007) should allow us to investigate the effect of different conformations of the β end rings on the colour of the crystals, to see whether this is a major factor in the bathochromic shift between free AXT and AXT in crustacyanin. In addition, we can compare each of these structures with those of free AXT as well as the AXT molecules bound in β-CR (PDB code 1GKA).

Fig. 4 shows that the polyene chains of s-*cis*-(1) and s-*trans*-(1) match very closely and likewise it was found that the polyene chains of the free AXT molecules (Bartalucci *et al.*, 2007) also align closely with that of s-*trans*-(1). However, a similar overlay of AXT1 from the protein crystal structure of β-CR [*i.e.* molecule (1) of the two AXT molecules in the β-CR structure] with s-*trans*-(1) shows that the r.m.s. deviation is 0.49 Å. Fig. 10(*a*) shows the overlay of the protein AXT1 represented in blue with s-*trans*-(1), in red, viewed down the plane of the polyene chains; the main differences arise from the distinct bowing of the polyene chain of AXT1 compared with that of s-*trans*-(1). Also, since AXT1 is the (3*R*,3′*R*) optical isomer of AXT, the end rings fit more closely with the higher-occupancy disordered component at one end of the centrosymmetric s-*trans*-(1), and more closely with the lower-occupancy disordered component at the other end; the $C2_{\text{s-}trans\text{-}(1)}$—C2 protein distance is 1.67 Å and the distance of $C2BA_{\text{s-}trans\text{-}(1)}$ to the equivalent protein atom, $C22_{\text{protein}}$ is 1.056 Å. These relatively large differences, also illustrated in Fig. 10(*b*), arise from the bowing of the polyene chain in AXT1 and obviously significantly increase the r.m.s. difference value to 0.49 Å.

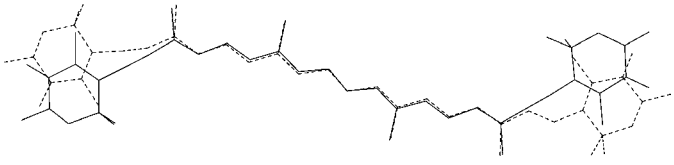

Figure 7
Overlay of the central part of the polyene chains of (3*S*,3′*S*)-7,8-didehydroastaxanthin (2) (dashed) and (3*S*,3′*S*)-7,8,7′,8′-tetradehydroastaxanthin (3) [excluding the lower-occupancy component disordered atoms of (2)] showing the quite different position of the end rings, and that they are s-*cis* and s-*trans*, respectively.

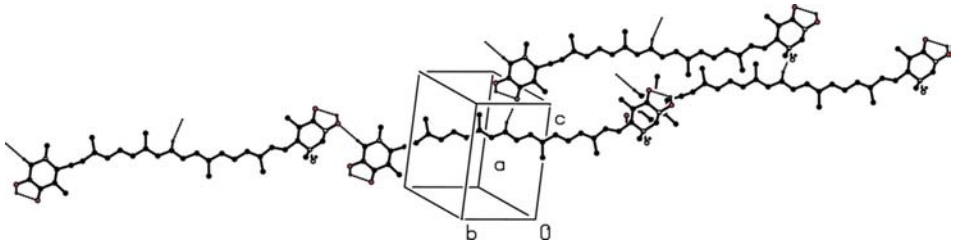

Figure 8
Packing of (3*S*,3′*S*)-7,8-didehydroastaxanthin (2), showing intermolecular C—H···O interactions; lower-occupancy disordered atoms are excluded and only H atoms involved in hydrogen bonding are shown.

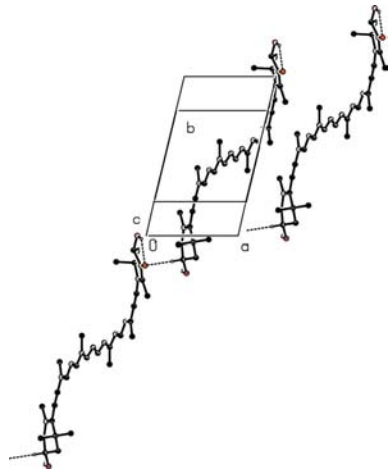

Figure 9
Packing of (3*S*,3′*S*)-7,8,7′,8′-tetradehydroastaxanthin (3) viewed approximately down **c**, showing intermolecular C—H···O and π-stacking interactions; only H atoms involved in hydrogen bonding are shown.

However, the conformation of s-*trans*-(1) is more similar to that of the protein-bound AXT molecules than any of the other free carotenoids, AXT, canthaxanthin and zeaxanthin, or of course the s-*cis*-(1), therefore, it was of interest to compare the colour of the crystals of s-*trans*-(1) and s-*cis*-(1). UV–vis spectra in the solid state were obtained from crystals pressed between two glass coverslips, and in the solution state in chloroform, Fig. 11. It should be noted that there is a solvent effect on the λ_{max} of carotenoids in solution, with a bathochromic shift of up to 20 nm in chloroform compared with solutions in hexane (Britton, 1995). Also, UV–vis spectra of samples in different states (aqueous buffer solution, organic solvents solution, or in the

solid state) are not directly comparable, but do reflect the different colour shades observed by the human eye. In chloroform solution, the λ_{max} is about 489 nm and s-*cis*-(1) was found to absorb at round about 500 nm, therefore, showing a small bathochromic shift compared with the solution-state spectrum. The solid-state spectrum of s-*trans*-(1) is very broad, and with some fine structure, with maxima at 513, 554 and 607 nm, which represents a definite bathochromic shift compared with the spectrum of s-*cis*-(1), as expected, due to an increase of the degree of conjugation of the polyene chain into the end rings.

The UV–vis spectra of a wide range carotenoids in the solution state have been compiled by Britton (1995). Comparisons of the UV–vis solution-state spectra of carotenoids having β end rings, with acyclic carotenoids containing the same number of conjugated double bonds, show a shift to shorter wavelength of *ca* 10 nm for each β end ring (Britton, 1995). Thus, lycopene, an acyclic carotenoid, β,ψ-carotene with one β end ring and β,β-carotene with two β end rings all potentially have 11 conjugated double bonds. However, the absorption maxima occur at 470, 461 and 450 nm, respectively, because the tilting of the β end rings in β,ψ-carotene and β,β-carotene reduces the degree of conjugation compared with the acyclic lycopene molecule, which is expected to be approximately planar. Adding a conjugated keto group at the 4-position of the β end group leads to a bathochromic shift of about 10 nm per keto group, so that the absorption maxima of β,β-carotene and canthaxanthin are 450 and 474 nm, respectively; adding a keto group in an acyclic carotenoid leads to a bathochromic shift of around 30 nm, with the effect of adding a second keto group giving rise to a reduced effect. Using these considerations, the absorption maximum for s-*cis*-(1) is expected to be similar to those of astaxanthin and canthaxathnin, at $\sim$ 480 to 490 nm (Bartalucci *et al.*, 2007) and a significant bathochromic shift of up to about 40–50 nm is expected for s-*trans*-(1), because the latter is planar. Although our solid-state spectra are very broad, the bathochromic shift expected between s-*cis*-(1) and s-*trans*-(1) has been confirmed. The s-*cis*-(1) spectrum is similar to that of AXT and canthaxanthin, with a single broad peak at 500 nm, whereas s-*trans*-(1) has a broad peak with fine structure, with the central peak occurring at $\sim$ 554 nm. Visually, the s-*trans*-(1) crystal appears to be a deeper, more purple–red colour than s-*cis*-(1), which is more orange–red in colour (see supplementary material). The fact that s-*cis*-(1) is solvated, whereas s-*trans*-(1) is not, may also contribute to the colour of the crystals. However, in Bartalucci *et al.* (2007) we were able to measure the UV–vis spectra of the chloroform solvate and unsolvated crystal forms of astaxanthin, which showed that the crystal colours were not significantly influenced by the incorporation of solvent, in that case. Another factor which could influence the colour of the β-CR protein is the fact that there is distinct bowing of the β-CR AXT polyene chains compared with that of s-*trans*-(1), but calculations suggest that this bowing will have a negligible effect on the colour (Durbeej & Eriksson, 2003, 2004).

The effect of replacing one or two double bonds with acetylenic groups as in (2) and (3) is expected to lead to absorption at a wavelength shorter by about 15 to 20 nm per acetylenic group added (Britton, 1995). However, this is counterbalanced by the fact that an acetylenic group added at the 7,8 position is likely to lead to coplanarization of the adjacent end ring, because of a reduction in steric hindrance between the end-ring methyl H atoms and the polyene chain due to a lack of a H atom bonded to C8. In fact, the crystal structure of (2) shows that both end rings are approximately coplanar with the polyene chain, even though the acetylenic group is only present next to one of the end rings, so the absorption spectrum of the crystals might be expected to absorb at longer wavelength than the solution. For (3), since the molecule in the crystal structure shows the end rings approximately coplanar with the polyene chain, which is also the conformation expected in solution because of the lack of H atoms at the 8 and 8′ positions, then the solution- and solid-state spectra are expected to be similar. In chloroform solution, the absorption maxima for (2) and (3) occur at 487 and 495 nm, respectively. The broad solid-state spectra obtained

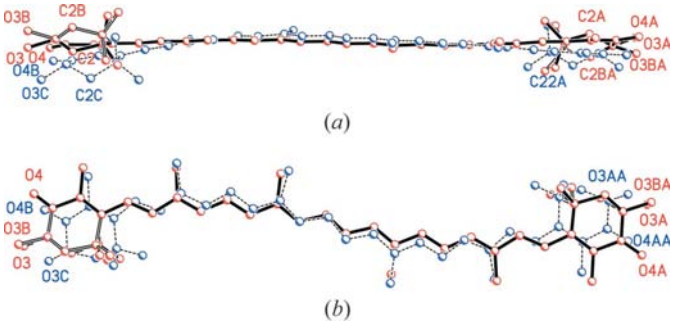

Figure 10
Comparison of the s-*trans* conformer of astaxanthin diacetate, s-*trans*-(1) (in red) with protein AXT1 [omitting the ester groups of s-*trans*-(1) for clarity]; (*a*) viewed down the plane of the polyene chain showing the bowing of the protein AXT1 polyene chain; (*b*) looking down on the polyene chain.

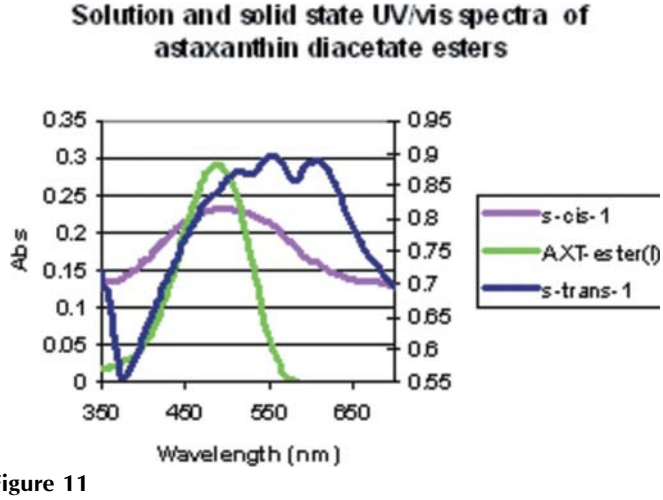

Figure 11
Solution-state (chloroform) UV–vis spectrum of the diacetate ester of astaxanthin and solid-state UV–vis spectra of the s-*cis* and s-*trans* conformers, s-*cis*-(1) and s-*trans*-(1).

for (2) and (3) are very similar to one another and also show the fine structure seen for s-*trans*-(1), with two shoulders at longer wavelength to the peak maxima. For (2), the λ_{max} values occur at about 495, 525 and 578 nm and for (3), the values are about 504, 542 and 584 nm, respectively (Fig. 12). Thus, although the solid-state spectra for (2) and (3) are very broad, making it difficult to draw conclusions, there do appear to be shifts to longer wavelengths, compared with the solution-state spectra for both (2) and (3). The peak maxima follow the order seen in solution, with a small bathochromic shift for (3) compared with (2), so that coplanarization of the end ring adjacent to the double bond in (2) has not had a significant impact. However, there is a significant shift to a longer wavelength for s-*trans*-(1) by 20–30 nm compared with the acetylenic derivatives, which is as expected because each acetylene linkage leads to a shift to shorter wavelength (Britton, 1995). Visually, the crystals of (2) and (3) appear very similar in colour to s-*trans*-(1). The fact that (2) adopts a 6-s-*cis* conformation whereas (3) adopts the 6-s-*trans* conformation of the end rings is not expected to lead to a significant shift in absorption maxima, although for acyclic carotenoids a reduction in absorbance may be seen for *cis* isomers.

The broadness of our solid-state spectra mean that small shifts in peak positions are difficult to determine precisely. Ideally, to obtain more accurate measurements of λ_{max} values for the crystal samples, we would like to measure our spectra by reflectance methods, directly from the crystals, a method which has been shown to produce high-quality spectra (Qi *et al.*, 2002; Ogawa *et al.*, 2004).

A variety of packing modes has been observed in the carotenoid crystal structures reported here, and those in Bartalucci *et al.* (2007). Intermolecular or intramolecular O—H···O hydrogen bonding was observed in the three crystal forms of AXT (Bartalucci *et al.*, 2007), and intramolecular O—H···O hydrogen bonding is seen for the acetylenic derivatives of AXT, (2) and (3) reported here. A suggested mechanism for the bathochromic shift seen in β-CR is that it arises from hydrogen bonding of the protein-bound AXT keto O atoms with a bound water molecule at one end of each AXT molecule and with a protonated histidine nitrogen at the other end, which causes a polarization effect along the polyene chain (Durbeej & Eriksson, 2003, 2004). Clearly the inter- and intramolecular hydrogen bonding to the keto oxygen seen in the crystal structures of the free carotenoids do not replicate the hydrogen bonding of the protein-bound AXT molecules, and as such, do not appear to affect the colours of the crystals. Likewise, various intermolecular distances between the polyene chains have been observed, from short distances suggestive of significant π-stacking of the polyene chains, to distances indicating predominantly van der Waals interactions, but again these interactions do not seem to affect the colour of the crystals significantly. Thus, this ensemble of crystal structures has not been able to mimic the situation seen in the β-CR where the proximity of the two AXT molecules to one another is proposed to lead to a strong exciton interaction, as another suggested mechanism for the bathochromic shift seen in β-CR (van Wijk *et al.*, 2005; Ilagan *et al.*, 2005). In β-CR the pairs of AXT molecules approach to a minimum distance of 7 Å and their angle to one another is about 120° (Cianci *et al.*, 2002), which we have not been able to mimic in our crystal structures thus far.

5. Conclusions

The ensemble of crystal structures reported here, together with those reported in Bartalucci *et al.* (2007), have allowed us to test the effect of carotenoid conformation, as well as the crystal-packing arrangements, and to some extent the effect of solvation, on the colours of the crystal. We have obtained crystal structures of a number of carotenoids with β end rings in the 6-s-*cis* conformation, with tilt angles of the end rings varying from −74.9 (3)° for zeaxanthin to 5.6 (1)° for 7,8-didehydroastaxanthin. We also have crystal structures of two carotenoids, s-*trans*-(1) and 7,8,7′,8′-tetradehydroastaxanthin (3), in the 6-s-*trans* conformation, both with end rings close to coplanar with the polyene chain [largest deviation of 13.3 (1)° for one end ring of (3)]. Although there is some variation in the colours of the crystals (see supplementary material), with

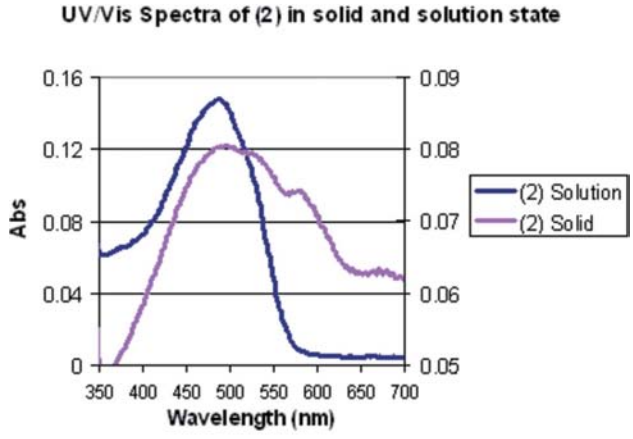

(*a*)

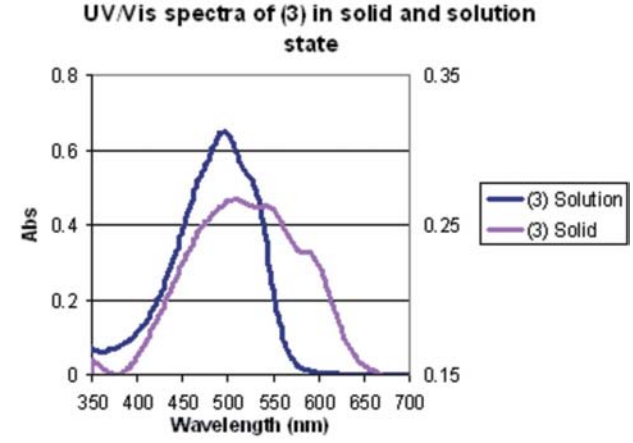

(*b*)

Figure 12
UV–vis spectra in chloroform solution and solid state (*a*) of (3*S*,3′*S*)-7,8-didehydroastaxanthin (2) and (*b*) of (3*S*,3′*S*)-7,8,7′,8′-tetradehydroastaxanthin (3).

the crystals of zeaxanthin appearing to be more orange, and s-*trans*-(1) appearing to be a deeper purple–red in colour, all the samples are definitely red in hue and not the blue colour of β-CR. The bathochromic shift of approximately 50 nm, seen in the solid-state spectrum of s-*trans*-(1), compared with that of s-*cis*-(1), can be attributed to the coplanarization of the end rings leading to an increase of conjugation. Thus, this ensemble of crystal structures has shown here that the effect of the end-ring conformation on the colour of the crystals is providing part of the overall bathochromic shift seen in the protein bound AXT in crustacyanin. This leads to the conclusion that one of the other colour-tuning mechanisms must be at work to produce the remainder of the bathochromic shift seen in α-CR and β-CR, namely polarization of the polyene chain caused by protonation of the keto O atoms or hydrogen bonding with the keto O atoms (Weesie *et al.*, 1997; Durbeej & Eriksson, 2003, 2004), and/or strong exciton coupling between the protein bound AXT molecules (van Wijk *et al.*, 2005; Ilagan *et al.*, 2005).

We acknowledge the support of an E.C. Marie Curie Fellowship to GB and a Nuffield Award to SF. Also, we thank STFC for our synchrotron beam time award on Station 9.8.

References

Bartalucci, G., Coppin, J., Fisher, S., Hall, G., Helliwell, J. R., Helliwell, M. & Liaaen-Jensen, S. (2007). *Acta Cryst.* B**63**, 328–337.
Bernhard, K., Kienzle, F., Mayer, H. & Müller, R. K. (1980). *Helv. Chim. Acta*, **63**, 1473–1490.
Britton G. (1995). *Carotenoids*, Vol. 1B, *Spectroscopy*, edited by G. Britton, S. Liaaen-Jensen & H. Pfander, ch. 2, pp. 13–44. Berlin: Birkhauser Verlag.
Bruker (2001*a*). *SMART*, Version 5.625. Bruker AXS Inc., Madison, Wisconsin, USA.
Bruker (2001*b*). *SADABS*, Version 2.03*a*. Bruker AXS Inc., Madison, Wisconsin, USA.
Bruker (2001*c*). *SHELXTL*, Version 6.12. Bruker AXS Inc., Madison, Wisconsin, USA.
Bruker (2002). *SAINT*, Version 6.36*a*. Bruker AXS Inc., Madison, Wisconsin, USA.
Chayen, N. E., Cianci, M., Grossmann, J. G., Habash, J., Helliwell, J. R., Nneji, G. A., Raftery, J., Rizkallah, P. J. & Zagalsky, P. F. (2003). *Acta Cryst.* D**59**, 2072–2082.
Cianci, M., Rizkallah, P. J., Olczak, A., Raftery, J., Chayen, N. E., Zagalsky, P. F. & Helliwell, J. R. (2002). *Proc. Natl. Acad. Sci.* **99**, 9795–9800.
Durbeej, B. & Eriksson, L. A. (2003). *Chem. Phys. Lett.* **375**, 30–38.
Durbeej, B. & Eriksson, L. A. (2004). *Phys. Chem. Chem. Phys.* **6**, 4190–4198.
Hashimoto, H., Yoda, T., Kobayashi, T. & Young, A. J. (2002). *J. Mol. Struct.* **604**, 125–146.
Ilagan, R. P., Christensen, R. L., Chapp, T. W., Gibson, G. N., Pascher, T., Polivka, T. & Frank, H. A. (2005). *J. Phys. Chem. A*, **109**, 3120–3127.
Karrer, P. & Jucker, E. (1950). *Carotenoids*, p. 235. Amsterdam: Elsevier Publishing Company Inc.
Nneji, G. A. & Chayen, N. E. (2004). *J. Appl. Cryst.* **37**, 502–503.
Ogawa, K., Harada, J., Fujiqara, T. & Takahashi, H. (2004). *Chem. Lett.* **33**, 1446–1447.
Qi, Z. M., Matsuda, N., Yoshida, T., Asano, H., Takatsu, A. & Kato, K. (2002). *Opt. Lett.* **27**, 2001–2003.
Sheldrick, G. M. (2008). *Acta Cryst.* A**64**, 112–122.
Spek, A. L. (2003). *J. Appl. Cryst.* **36**, 7–13.
Weesie, R. J., Verel, R., Jansen, F. J. H. M., Britton, G., Lugtenburg, J. & deGroot, H. J. M. (1997). *Pure Appl. Chem.* **69**, 2085–2090.
Wijk, A. A. C. van, Spaans, A., Uzunbajakava, N., Otto, C., de Groot, H. J. M., Lugtenburg, J. & Buda, F. (2005). *J. Am. Chem. Soc.* **127**, 1438–1445.
Zagalsky, P. F. (2003). *Acta Cryst.* D**59**, 1529–1531.